JMEPEG
https://doi.org/10.1007/s11665-022-07095-7

1059-9495/$19.00

TECHNICAL ARTICLE

Empirical Modeling of Microstructural and Hardness Characteristics of Severely Deformed 7075 Aluminum Alloy in the Semi-Solid State Using Response Surface Methodology

Ramin Meshkabadi and Vahid Pouyafar

Submitted: 4 March 2022 / Accepted: 14 May 2022

The microstructure and hardness of severely deformed 7075 aluminum alloy by equal channel angular pressing (ECAP) method in the semi-solid state were statistically investigated. The studied responses are grain size, shape factor, and hardness of primary α-Al grains in the semi-solid state. The response surface methodology (RSM) based on Box–Behnken design (BBD) was used to study the influence of ECAP passes, reheating temperature, and holding time on the responses. Mathematical relationships between the input variables and the responses were developed using the analysis of variance (ANOVA). Analysis of residuals versus run number and comparison between the measured and predicted results showed that all three developed models could predict the responses adequately. The calculated percentage contribution of input variables showed that the holding time is the main factor, followed by reheating temperature influenced the microstructural characteristics. The hardness of semi-solid samples was influenced principally by the number of ECAP passes and in the second level by the holding time.

Keywords 7075 aluminum alloy, equal channel angular pressing, response surface methodology, semi-solid metal feedstock

1. Introduction

Semi-solid forming process, first discovered at the Massachusetts Institute of Technology (MIT), is one of the forming methods of metals and alloys in the semi-solid region (Ref 1). This process has advantages such as better die filling, reduced air entrapment, and shrinkage porosities compared with traditional casting, along with reduced forming forces and production costs in comparison with traditional forging techniques (Ref 2, 3). It is a three-step process: the production of a semi-solid billet, semi-solid heating, and the forming process.

The spherical solid phase dispersed among the liquid phase results in the more effortless material flow in semi-solid forming. So, the development of this technology depends on the production of feedstock with a spherical microstructure. There are several methods to obtain such a spherical microstructure, including mechanical stirring, magnetohydrodynamic stirring (MHD), grain refinement, and thermomechanical methods (Ref 4).

Ramin Meshkabadi, Department of Engineering Sciences, Faculty of Advanced Technologies, University of Mohaghegh Ardabili, Namin, Iran; and **Vahid Pouyafar**, Manufacturing Engineering Department, University of Tabriz, Tabriz, Iran. Contact e-mail: r_meshkabadi@uma.ac.ir.

Thermomechanical methods are a kind of solid-state method based on applying critical strain on the material to stimulate the recrystallization process. One of these methods is the strain-induced melt activation (SIMA) process, consisting of cold deformation to store strain on the material and then semi-solid reheating. This method is very suitable for aluminum and magnesium alloys (Ref 5). Recently, severe plastic deformation (SPD) has developed to impose extensive strains on the material (Ref 6, 7). SPD procedures such as equal channel angular pressing (ECAP) have more tremendous potential for industrial applications. They have two significant advantages over conventional methods like extrusion. Firstly, the applied strains are homogeneous. Secondly, the dimensions of the sample do not change by applying multiple passes (Ref 8, 9). In the SIMA route, some factors affect the microstructural characteristics and mechanical properties of the material at a semi-solid temperature. These factors include those affecting the rate and the homogeneity of the initial strain and factors related to the subsequent reheating.

Various studies have suggested using SPD methods for successful semi-solid billet production. Moradi et al. (Ref 10) employed a thermomechanical treatment method by using ECAP at the ambient temperature to produce feedstock for semi-solid forming. The results indicated that ECAP followed by semi-solid reheating was an effective method to produce semi-solid ingot for thixoforming. Fu et al. (Ref 11) introduced a modified SIMA route based on the ECAP method to prepare a semi-solid slurry and investigated the microstructural changes. The results indicated that as the applied strain increased, the grain size decreased, and more spherical grains were obtained. Ashouri et al. (Ref 12) utilized ECAP for one to four passes to induce a great strain and examined the effect of strain on the morphology and shape factor of reheated alloy in

Published online: 28 June 2022

the semi-solid region. They concluded that with the increase in strain, the particles sphericity increases, their size will decrease, and sphericity takes place in less reheating time.

In a study by Meshkabadi et al. (Ref 13), the microstructure of a semi-solid 7075 aluminum alloy severely deformed by the ECAP route was investigated through the design of experiment using the Taguchi approach. The results showed that grain size was more affected by processing route and holding time at semi-solid temperature. The sphericity of the grains was more affected by the processing routes, holding time, and forming temperature.

In other studies on 7075 Aluminum alloy, the influences of the initial strain and semi-solid heating parameters on microstructural characteristics have been investigated. These include the effects of strain inducing and heating conditions on the resultant microstructure (Ref 14), recrystallization mechanism in the semi-solid temperature (Ref 15), the effect of strain rate on microstructural evolution of the material (Ref 16-18), the effect of reheating temperature and holding time on the formation of a suitable semi-solid feedstock (Ref 19), the effects of the isothermal holding process on the microstructure evolution of the semi-solid alloy (Ref 20), the effects of the number of ECAP passes on the morphology and shape factor (Ref 12) and the effects of parallel tubular channel angular pressing (PTCAP) parameters on microstructure and homogeneity of tubes in the semi-solid region (Ref 21).

As is well known, the presence of dispersed fine precipitates in the microstructure of 7075 aluminum alloy makes it difficult to recrystallize in the solid state. The pinning effect prevents the movement of dislocations. Therefore, the semi-solid forming of this alloy has been considered in recent years (Ref 15). According to the previous studies, it is challenging to impose cold work on wrought aluminum alloys at room temperature because it leads to crack formation and abrupt breakdown (Ref 22). In 7075 alloy, some fine precipitates such as $Al_3Zn_3Mg_3$ and $MgZn_2$ are formed by the decomposition of a supersaturated solid solution during age hardening (Ref 15). These fine intermetallic particles cause the sample's breakdown during the process (Ref 22). To avoid crack formation during the process, it is essential to perform appropriate heat treatment prior to the ECAP to reduce their hardness. In a conducted research by Fallahi et al. (Ref 23), the effects of pre-ECAP heat treatment on the success of the process were investigated by performing annealing and solution heat treatments. The results indicated that the annealing heat treatment at 320 °C for two hours and furnace cooling reduced the hardness value significantly and the material became softer.

The reasons for performing this study are the shortcomings of previous research. The simultaneous and combined effects of the effective parameters in the final microstructure and hardness characteristics are not addressed. When only one parameter is changed, other inputs are held constant. As a result, this method does not reveal the full effect of inputs on the response. The increased number of experiments leads to an increase in time and expenses. It is one of the other limitations of such studies. In order to overcome these problems and describe the process with a high degree of accuracy, the simultaneous effects of independent variables on the process output should be considered. In these situations, a multivariate statistical technique like response surface methodology (RSM) is the solution. Response surface methodology is a statistical method for modeling a process by fitting a mathematical equation on the experimental data. It describes the significance of each of the input parameters and develops the relationships between them and responses.

The main objective of this study is to gain further insight into the process-structure-property correlations and relate the various input parameters to microstructure and hardness, through the response surface methodology for better feedstock production. The interaction effects between process parameters and the significance of each of them are investigated in this research. The number of ECAP passes, holding time, and heating temperature are the three main factors in the experiment. The grain size (G_s), shape factor (S_f), and hardness number (HRB) of primary α-Al grains were adopted as responses to evaluate the slurry production criteria. For this purpose, the Box–Behnken design (BBD) was used for designing the experiments. So far, such a statistical survey of the production process of appropriate feedstock via the SIMA route has not been reported in the literature. Proper selection of effective parameters in achieving the appropriate semi-solid microstructure will make the industries benefit from the production of high-quality and low-cost complex parts compared to the traditional casting method.

2. Experimental Procedure

Chemical compositions (via quantometer analysis) of the as-received 7075 aluminum alloy in wt.% were Al-5.27Zn-2.25Mg-1.51Cu-0.405Fe-0.333Si. The solidus and liquidus temperatures are 540°C to 650 °C, accordingly. For the ECAP process, a die containing channels with the same cross-section area was designed, as illustrated in Fig. 1. The channel diameter was 20 mm, the angle of the die was $\phi = 90^\circ$ and the outer curvature angle was $\psi = 20^\circ$. In Fig. 2, the cracking of this alloy is shown after the ECAP process at room temperature.

The practical experiments of this study confirm the concluded results by Fallahi et al. (Ref 22), where the ECAP process on the solution treated samples (490 °C for 5 h and then water quench) led to the appearance of the cracks in the first pass (Fig. 3a). In the annealed sample, no cracks could be observed even in the subsequent passes, as shown in Fig. 3(b).

The pressing was performed at room temperature with the speed of 10 mm/s and by spraying MoS_2 inside the die to reduce the friction between the die wall and sample. As previously proved, the applied strain in route B_A is more homogeneous than other ECAP routes (Ref 24), so that the ECAP was performed on the successive passes in this route.

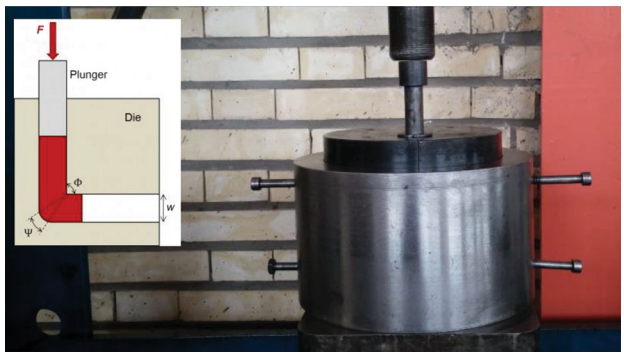

Fig. 1 Designed die and related angles

For reheating, a resistance furnace was used and the sample's temperature was controlled by a K-type thermocouple. The ECAP-treated samples were heated to the semi-solid temperature (610, 615 and 620 °C) and then were held for (5, 10 and 15 min). The samples were quenched quickly in water, and their microstructure was examined by optical microscopy. The quenched specimen was ground, polished and then etched using Keller's reagent. The microstructure characteristics (grain size (G_s) and shape factor (S_f)) were calculated using Eq 1 and 2.

$$G_s = \frac{\sum_1^N \sqrt{4A/\pi}}{N} \quad \text{(Eq 1)}$$

$$S_f = \frac{1}{\left(\sum_1^N P^2/4\pi A\right)/N} \quad \text{(Eq 2)}$$

where A and P are the surface area and perimeter of the particle obtained using Clemex image analyzer software, and N is the number of particles in a specified region (Ref 12). The hardness testing is conducted to the Rockwell B scale (model DuraJet G5 made by EMCO-TEST (Austria)) according to regulation of ASTM E-18. It incorporates a steel ball, with a load of 100 kg for a dwell time of 10 s.

Fig. 2 Cracked sample after performing the ECAP process at room temperature

3. Design of Experiments

An appropriate billet for the semi-solid forming process should have a spherical microstructure. It depends on the strain-inducing factors and the parameters of the subsequent semi-solid heating. The number of ECAP passes (N_P), reheating temperature (T_r) and holding time (T_h) were defined as independent input parameters. The desired responses were the grain size (G_s), shape factor (S_f) and the hardness number (HRB). In the RSM, the overall model of the prediction function of the response (Y) based on the input parameters (N_P, T_r and T_h) is expressed in the following:

$$Y = f(N_P, T_r, T_h) \quad \text{(Eq 3)}$$

where f is the response function and Y is the desired response value. In order to predict the response (Y) as a function of independent factors and their interactions, a polynomial equation (Eq. 4) Containing the quadratic terms was proposed.

$$Y = \beta_0 + \sum_{i=1}^{3} \beta_i X_i + \sum_{i=1}^{3} \beta_{ii} X_i^2 + \sum_{i<j}^{3} \beta_{ij} X_i X_j \quad \text{(Eq 4)}$$

where β_0, β_i, β_{ii} and β_{ij} are constant, linear, quadratic and interaction regression coefficient terms, respectively; X_i and X_j are independent factors. The following equation can be applied to transform an absolute value (z_i) into a coded value (X_i) according to a determinate experimental design:

$$X_i = \left(\frac{z_i - z_i^0}{\Delta z_i}\right) \quad \text{(Eq 5)}$$

where Δz_i is the distance between the actual value in the central point and the actual value in the superior level and z^0 is the real value of the central point.

Fig. 3 ECAP-treated samples after (a) solution treatment and appeared cracks for one-pass and (b) Annealing treatment for 1, 2, and 3 passes without any cracks

Table 1 Input parameters and their levels

Parameter	Unit	Levels		
		–1	0	1
Number of ECAP passes	–	2	3	4
Reheating temperature	°C	610	615	620
Holding time	Min	5	10	15

In this study, the collection of experimental data adopted the Box–Behnken design (BBD). It consists of 15 experiments for developing the regression model to predict the response value. The software program used was Stat-Ease Design Expert (DX8). The levels of the three factors on ECAP and reheating parameters are reported in Table 1. A schematic representation of the experimental procedures indicating all the processing stages and conditions is shown in Fig. 4.

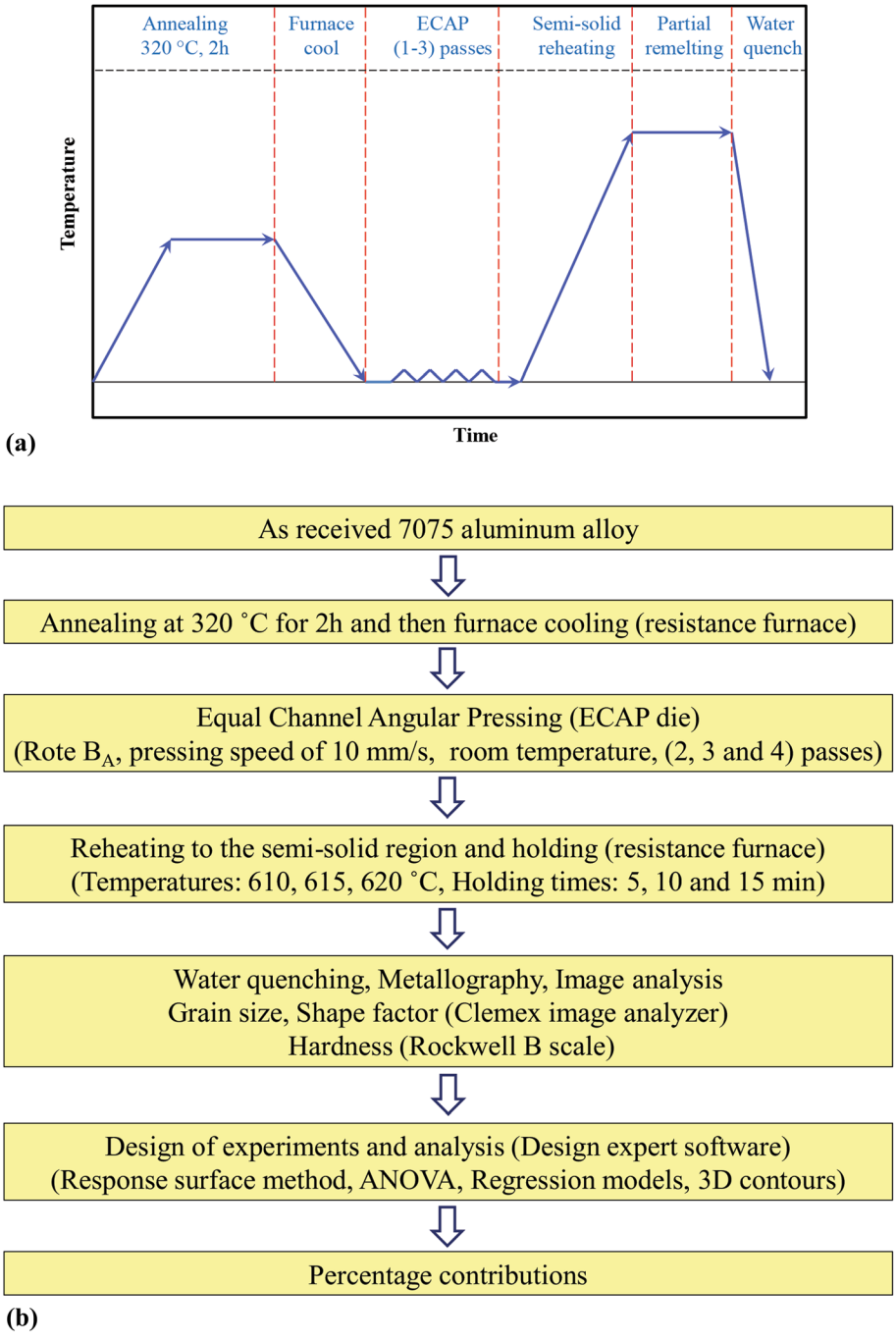

Fig. 4 (a) A schematic representation of the experimental procedures and (b) the processing stages and conditions

4. Results and Discussion

The 15 experiments were carried out according to the conditions in Table 2. The obtained microstructures corresponding to 15 runs are illustrated in Fig. 5. The grain size, shape factor, and hardness values were measured at least in 5 different points, and the average values were tabulated in Table 2. Significance tests of the regression models, significance tests on model coefficients and tests for lack of fit are necessary for model adequacy checking (Ref 25). Analysis of variance (ANOVA) has been carried out for this purpose.

4.1 Analysis of Grain Size

The grain size is one of the most critical parameters that play a significant role in the semi-solid forming process. Recent research results show that the suitable grain size range for semi-solid processes is 70-100 μm (Ref 26). The fit summary suggested that the quadratic model is statistically significant for the grain size analysis. The summary table of ANOVA for grain size is given in Table 3.

For a well-fitted model, the determination coefficient (R^2) should not be less than 80%. When R^2 approaches unity, it indicates that the response equation gives a good fit for the actual data. It is common to use the adjusted R2 coefficient to determine how well the model fits the data.

The value of R^2= 0.9944 represents that 99.44% of the total variations can be predicted using the fitted model. The value of the adjusted R^2= 0.9844 shows that 98.44% of the total variations can be predicted by employing a regression model that contains significant parameters. The value of R^2 and adjusted R^2 is over 98%. It means that the regression model can reasonably predict the relationship between the independent factors and the final response. The corresponding p value for the model is less than 0.05 (i.e., α = 0.05, or 95% confidence level), and the model f value is 99.47, which indicates that the model is statistically significant (Ref 25). Adequate precision measures the signal-to-noise ratio. A ratio greater than 4 is desirable. The ratio of 34.478 indicates an adequate signal. The "Lack of Fit F value" of 4.75 implies that the Lack of Fit is not significant and there is a 17.88% chance that a "Lack of Fit F value" could occur due to noise. The lack of fit term is non-significant as we desire.

Table 3 shows the significant and standard errors of each coefficient. They were also determined by values of "F value"' and "Prob. > F" for the fitted models. For grain size (G_s), among the first-order parameters, the X_1 (N_p), X_2 (T_r), and X_3 (T_h), the second-order parameters X_2^2 and the interactive parameters X_2X_3 are found to be the significant terms because of their "Prob. > F" value being less than 0.05. In the same way, the terms X_1X_2, X_1X_3, X_1^2, and X_3^2 are insignificant. Eq 6 presents the final quadratic model of the response equation for grain size in terms of coded factors.

$$G_s = 80.00 + 3.12X_1 - 11.50X_2 + 13.88X_3 + 1.50X_1X_2 + 1.75X_{-1}X3 - 6.00X_2X_3 - 2.12X_1^2 - 3.87X_2^2 - 0.63X_3^2 \quad \text{(Eq 6)}$$

Figure 6(a) shows the differences between actual and predicted values. The predicted values have a slight difference with the measured values of the tests and represent the high accuracy of the model. Figure 6(b) illustrates the internally studentized residuals versus the run number. The differences between the actual and the predicted responses are in the acceptable limit in the context of internally studentized residuals.

Table 2 Design of experimental matrix and obtained results

Run no.	Coded factors			Actual factors			Responses		
	X1	X2	X3	NP	Tr	Th	Gs	Sf	HRB
1	1	1	0	4	620	10	69	0.63	47
2	0	0	0	3	615	10	79	0.59	45
3	− 1	0	− 1	2	615	5	63	0.53	39
4	0	1	1	3	620	15	71	0.84	47
5	0	0	0	3	615	10	81	0.61	44
6	0	− 1	− 1	3	61	5	68	0.51	43
7	1	0	− 1	4	615	5	64	0.49	51
8	0	1	− 1	3	620	5	55	0.67	41
9	0	− 1	1	3	610	15	108	0.69	58
10	− 1	− 1	0	2	610	10	82	0.58	44
11	1	− 1	0	4	610	10	87	0.54	58
12	1	0	1	4	615	15	95	0.67	59
13	− 1	0	1	2	615	15	87	0.71	46
14	0	0	0	3	615	10	80	0.59	45
15	− 1	1	0	2	620	10	58	0.78	40

In order to investigate the influences of the number of ECAP passes and semi-solid reheating factors on the grain size (Gs), the three-dimensional response surfaces are drawn in Fig. 7.

Referring to Fig. 7(a), when the holding time stays at its center level, with increasing the reheating temperature, the grain size decreases significantly, while with increasing the number of ECAP passes, no appreciable change in the grain size is observed and it is reduced slightly. According to Fig. 7(b), when the reheating temperature (Tr) is kept at its center levels, the increase in the number of applied passes does not affect the grain size, while it increases with increasing the holding time in the semi-solid temperature. Figure 7(c) shows that, in the constant level of the number of ECAP passes, the grain size increases with increasing holding time, faster at the lower heating temperatures, while no significant change is observed at high reheating temperatures. Also, with increasing the reheating temperature and especially at low holding times, the grain size is almost constant, but the size of the grains shows a decreasing trend with increasing holding time.

The dimensional response surface illustrates that the number of ECAP passes has the most negligible effect on the grain size of the semi-solid phase. In the SIMA process, applying the cold work is necessary to store the energy needed for the recrystallization process in the semi-solid zone. According to previous studies, the amount of stored strain energy has a critical value in which storing more than that critical value does not contribute on the recrystallization process. According to the research carried out by Bolouri et al. (Ref 17), the amount of needed cold work for the 7075 aluminum alloy is about 30%. This amount of required cold work in comparison with the amount of cold work per ECAP pass (which is 100%) can confirm the results obtained in the research, in that the increase in the number of ECAP passes does not affect the recrystallization process and the resulting size of the grains.

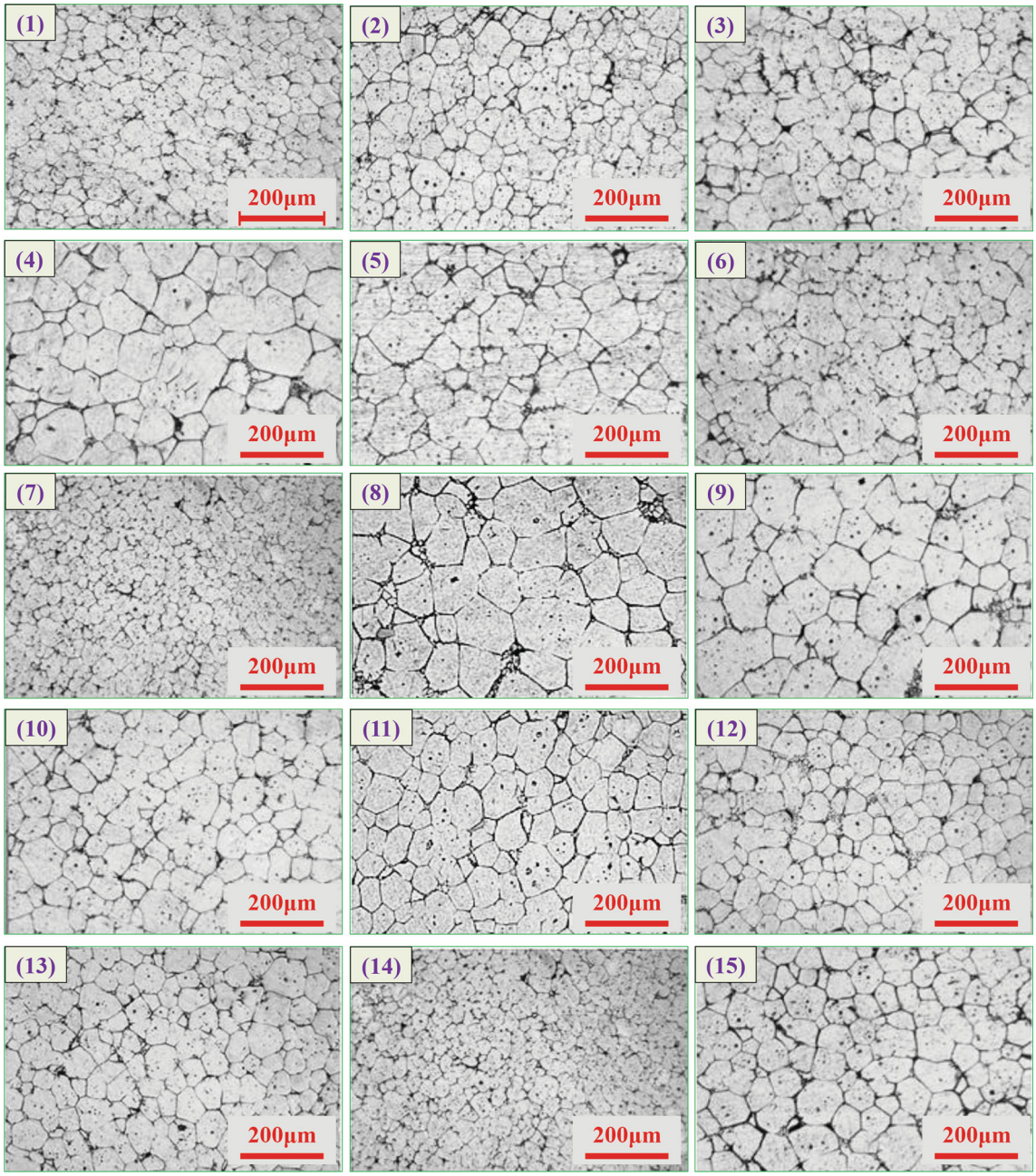

Fig. 5 The microstructure of the 15 experiments according to conditions in Table 2

By examining Fig. 6, it is observed that the holding time in the semi-solid range (regardless of the number of applied passes and the reheating temperature) has the most significant effect on the size of the solid phase. As the holding time increases, the grain size increases as the sharp edges disappear and the surface energy of the solid particles decreases (Ref 12). As the holding time increases, the liquid phase between the solid grains thickens and its fraction increases. As a consequence, the Ostwald ripening mechanism, which has been active for a long time, can be considered as a dominant mechanism of grain growth (Ref 27, 28). These trends were also observed in obtaining a semi-solid feedstock by Mohammadi et al. (Ref 19) and Wang et al. (Ref 20) by the RAP method and by Meshkabadi et al. (Ref 21) by the SIMA route.

4.2 Analysis of Shape Factor

The statistical significance of the fitted quadratic model for the shape factor is evaluated by the P values of ANOVA, and Table 4 shows the results.

The value of R^2= 0.9867 represents that 98.67% of the total variations is predictable using the fitted model. The value of the adjusted R^2= 0.9626 shows that 96.26% of the total variations can be predicted by employing a regression model that contains significant parameters. The value of R^2 and adjusted R^2 is over

Table 3 ANOVA table for grain size

Source	Sum of squares	df	Mean square	f value	Prob > f
Model	2909.48	9	323.28	99.47	< 0.0001
X_1	78.13	1	78.13	24.04	0.0045
X_2	1058.00	1	1058.00	325.54	< 0.0001
X_3	1540.12	1	1540.12	473.88	< 0.0001
X_1X_2	9.00	1	9.00	2.77	0.1570
X_1X_3	12.25	1	12.25	3.77	0.1099
X_2X_3	144.00	1	144.00	44.31	0.0012
X_1^2	16.67	1	16.67	5.13	0.0729
X_2^2	55.44	1	55.44	17.06	0.0091
X_3^2	1.44	1	1.44	0.44	0.5348
Residual	16.25	5	3.25		
Lack of Fit	14.25	3	4.75	4.75	0.1788
Pure Error	2.00	2	1.00		
Cor. Total	2925.73	14			

R^2= 0.9944, adjusted R^2 =0.9844, predicted R^2=0.9205, adequate precision= 34.478.

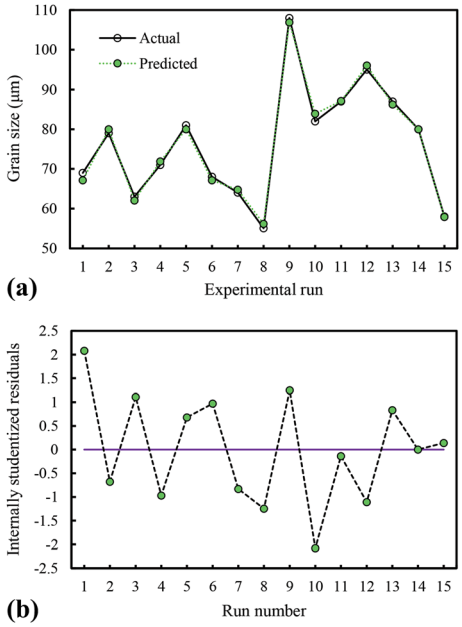

Fig. 6 (a) The comparison between actual and predicted values and (b) Residuals versus run number for the grain size

96%. This means that the regression model predicts the relationship between the independent factors and the final response. The p value for the model term is less than 0.05 (i.e., α = 0.05, or 95% confidence level) and the model f value is 41.07, which indicates that the model is statistically significant. The ratio of 23.053 for adequate precision indicates an adequate signal. The "Lack of Fit F value" of 3.94 implies the Lack of Fit is not significant and there is a 20.91% chance that a "Lack of Fit F value" could occur due to noise. The lack of fit term is non-significant as we desire.

Table 4 shows the significance of each factor for the fitted model determined by the values of "F value"' and "Prob. > F". From Table 4, it is realized that X_1 (N_p), X_2 (T_r), X_3 (T_h), X_1X_2, and X_2^2 have statistical significance on the shape factor, whereas X_1X_3, X_2X_3, X_1^2, and X_3^2 are insignificant. Eq (7) represents the developed regression model equation for the shape factor from the above functional relationship.

$$G_s = 0.6 - 0.034X_1 + 0.075X_2 + 0.089X_3 - 0.027X_1X_2 - 0.0025X_2X_3 - 0.021X_1^2 + 0.057X_2^2 + 0.024X_3^2 \quad \text{(Eq 7)}$$

The predicted values of shape factor (S_f) are obtained from the regression equation and compared with the corresponding experimental values (Fig. 8a). The predicted values slightly deviate from the experimental values. Figure 8(b) clearly shows that the distribution of the internally studentized residuals for the shape factor approximately follows the fitted normal distribution.

Figure 9 shows the 3D surface graphs for the shape factor are shown. These 3D surface graphs estimate the shape factor values for any combination of the input variables.

In Fig. 9(a), when the holding time remains constant at the center level, the shape factor does not change with the increase in the number of ECAP passes, while it increases significantly with increasing the reheating temperature in the semi-solid range. Figure 9(b) shows that when the heating temperature stays constant, increasing the number of passes has no significant effect on the shape factor, while the prolongation of the holding time improves the shape factor at that temperature. It can be deduced from Fig. 9(c) that when the number of passes is kept at its center level, the value of the shape factor increases with increasing both the reheating temperature and holding time. In this case, the parameters of the semi-solid heat treatment have a cumulative effect on the shape factor.

From Fig. 9(a) and (c), by increasing the reheating temperature, the values of shape factor improve. It is due to the effect of interface curvatures. With increasing temperature and the formation of a sufficient liquid phase, the liquid phase penetrates the high-energy boundaries and converts the previous grains into coaxial and spherical grains (Ref 18). However, the holding time has a significant impact because when it increases, the surface energy between the solid particles decreases and the sharp edges disappear. From the literature discussion, it can be known that by increasing the holding

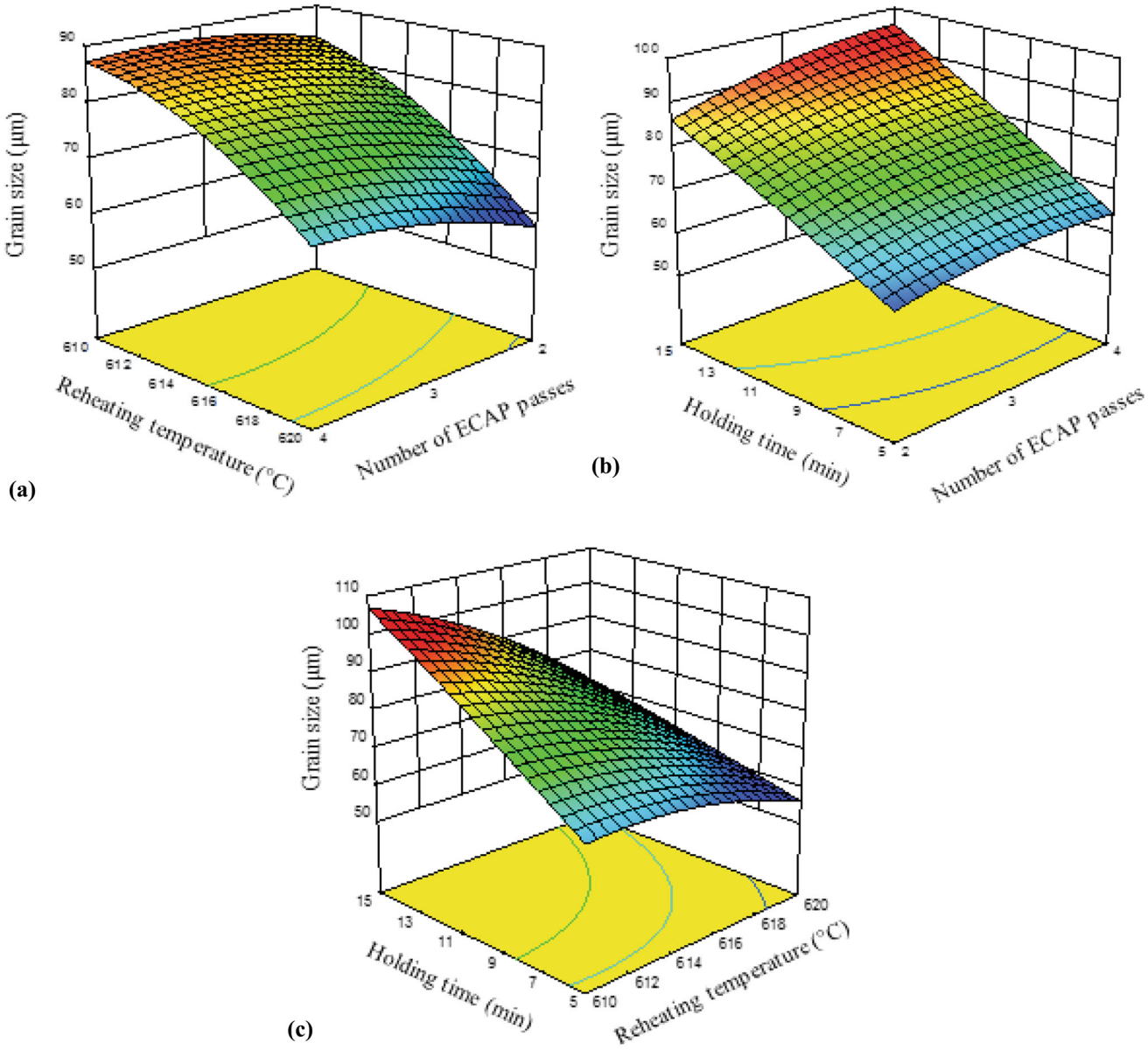

Fig. 7 Response surface plots showing the effects of (a) the number of ECAP passes and reheating temperature, (b) the number of ECAP passes and holding time, and (c) reheating temperature and holding time on grain size

period, the evolution mainly includes the increase in liquid content, structural separation and grain globularization. In short periods, thin liquid films have separated the initial grains due to the low liquid fraction. In such a system, the grains can easily connect and coarsen. Besides that, the Ostwald ripening mechanism is also active because the distance between the grains is minimal. At the same time, by increasing the liquid phase, there is also a reluctance to separate the connected grains. The activation energy of this stage is provided by increasing the amount of the liquid phase (Ref 29). As the

Table 4 ANOVA table for shape factor

Source	Sum of squares	df	Mean square	*f* value	Prob > *f*
Model	0.14000	9	0.01500	41.07	0.0004
X_1	0.00911	1	0.00911	24.74	0.0042
X_2	0.04500	1	0.04500	122.17	0.0001
X_3	0.06300	1	0.06300	171.07	< 0.0001
X_1X_2	0.00302	1	0.00302	8.21	0.0352
X_1X_3	0.00000	1	0.00000	0.000	1.0000
X_2X_3	0.00002	1	0.00002	0.068	0.8048
X_1^2	0.00160	1	0.00160	4.35	0.0914
X_2^2	0.01200	1	0.01200	32.19	0.0024
X_3^2	0.00215	1	0.00215	5.85	0.0601
Residual	0.00184	5	0.00036		
Lack of Fit	0.00157	3	0.00052	3.94	0.2091
Pure Error	0.00026	2	0.00013		
Cor. Total	0.14000	14			

R^2= 0.9867, adjusted R^2 =0.9626, predicted R^2=0.8130, adequate precision= 23.053.

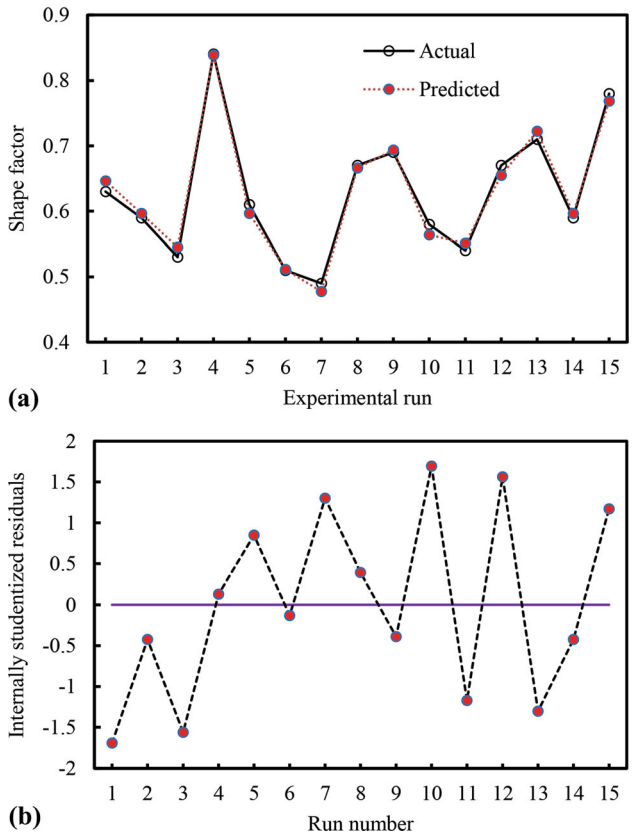

Fig. 8 (a) The comparison between actual and predicted values and (b) Residuals vs. run number for the shape factor

heating time prolongs, the liquid content increases and the coarsening relatively weakens. In addition, the coalescence makes the grains irregular and thus, the shape factor increases sharply.

4.3 Analysis of Hardness

The ANOVA table of the quadratic model with other adequacy measures for hardness investigation is given in Table 5.

The associated *p* value of less than 0.05 for the model (i.e., α = 0.05, or 95% confidence level) indicates that the model terms are statistically significant. The lack of fit value of the model is 7, indicating that there is a 12.76% chance that a "Lack of Fit *F* value" could occur due to noise. It implies non-significance, as this is desirable. The other adequacy measures including R^2, adjusted R^2, predicted R^2 are close to 1 and in a reasonable agreement, which indicates the model's adequacy. The value of an adequate precision rate of 20.276 indicates good model discrimination. The ANOVA result shows the terms X_1 (N_p), X_2 (T_r), X_3 (T_h), X_1X_2, X_2X_3, X_1^2, and X_3^2 are the significant model terms associated with hardness. The other model terms, including X_1X_3 and X_2^2, are not significant.

Regarding the effective parameters and obtained coefficients, the final mathematical model of hardness used for prediction within the same design space is given as Eq. 8.

$$HRB = 44.67 + 5.75X_1 - 3.5X_2 + 4.5X_3 - 1.75X_1X_2 + 0.25X_1X_3 - 2.25X_2X_3 + 2.04X_1^2 + 0.54X_2^2 + 2.04X_3^2 \quad \text{(Eq 8)}$$

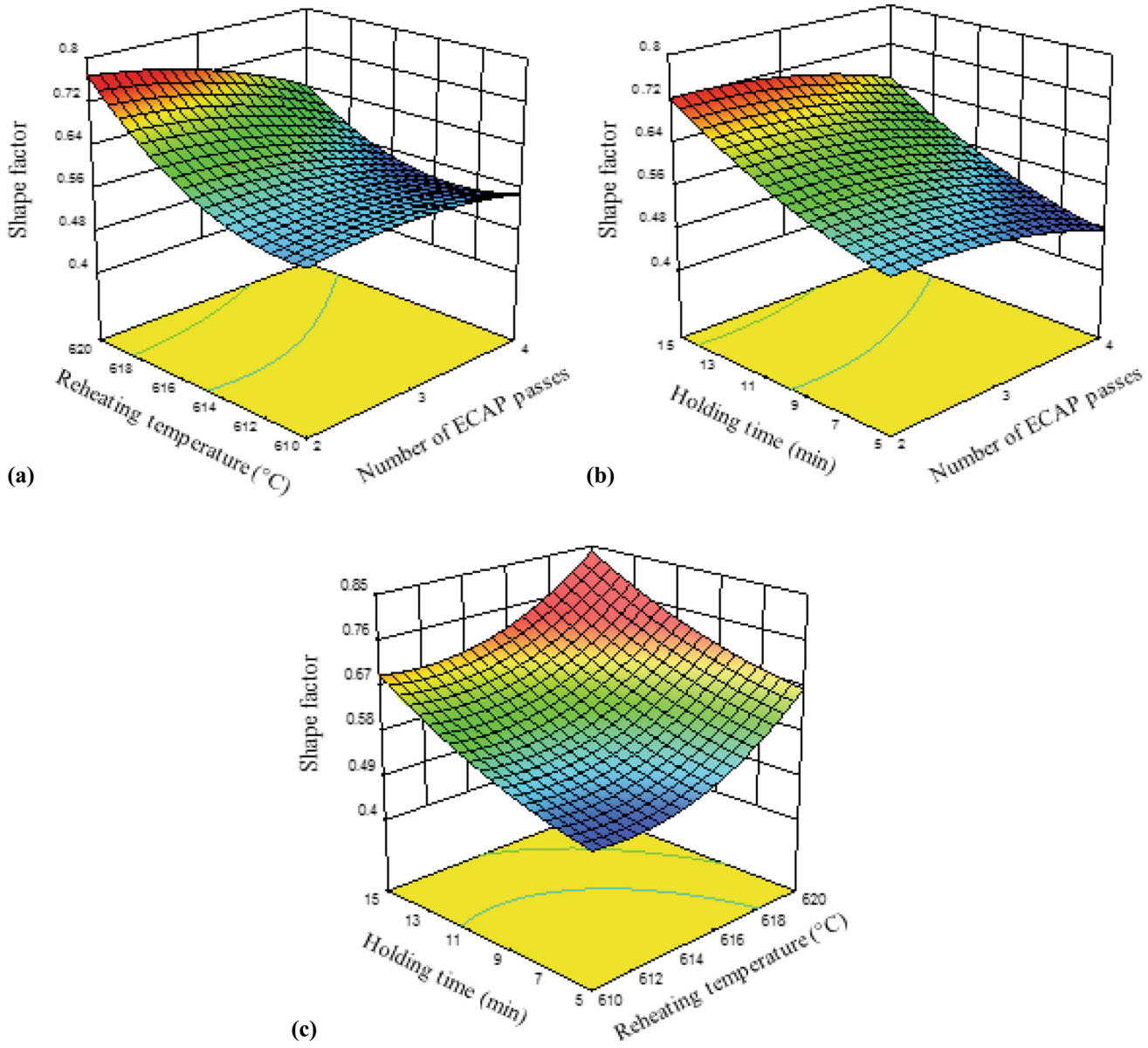

Fig. 9 Response surface plots showing the effects of (a) the number of ECAP passes and reheating temperature (b) the number of ECAP passes and holding time and (c) reheating temperature and holding time on shape factor

Figure 10 shows the relationship between the actual and predicted values of hardness. It illustrates that the developed model is adequate and predicted results are consistent with measured values. Figure 10(b) exhibits a random scatter on the residuals versus the run number. It ensures that the performed experiments are appropriate for the design of experiment process.

In terms of interaction between the number of ECAP passes and reheating temperature, as shown in Fig. 11(a), it is evident that hardness value tends to increase with lower reheating temperature and more ECAP passes.

Figure 11(b) shows the interaction of the number of ECAP passes and holding time on the hardness value. It is evident that increasing the number of ECAP passes and increasing the holding time in the semi-solid temperature increases the hardness. At a fixed level of reheating temperature, by increasing the holding time, solid solution hardening of 7075 aluminum alloy by secondary solid elements, which occurs at higher temperature and time, may lead to an increase in the hardness value (Ref 30).

Figure 11(c) represents the interaction of reheating temperature and holding time on the hardness of the semi-solid alloy. In this case, the highest hardness occurs at lower reheating temperatures and more holding time. As the temperature rises and the recrystallization continues, many of the dislocations and remaining residual stresses from cold work are solved and the resistance to the motion of dislocations is reduced (Ref 30). These reasons reduce the hardness values at elevated temperatures.

4.4 Percentage Contribution of Input Parameters on the Responses

One of the best ways to express the degrees of importance of the significant parameters is to calculate the percentage of

Table 5 ANOVA table for hardness

Source	Sum of squares	df	Mean square	*f* value	Prob > *f*
Model	586.07	9	65.12	42.47	0.0003
X_1	264.50	1	264.50	172.50	< 0.0001
X_2	98.00	1	98.00	63.91	0.0005
X_3	162.00	1	162.00	105.65	0.0001
X_1X_2	12.25	1	12.25	7.99	0.0368
X_1X_3	0.25	1	0.25	0.16	0.7031
X_2X_3	20.25	1	20.25	13.21	0.0150
X_1^2	15.39	1	15.39	10.04	0.0249
X_2^2	1.08	1	1.08	0.71	0.4389
X_3^2	15.39	1	15.39	10.04	0.0249
Residual	7.67	5	1.53		
Lack of Fit	7.00	3	2.33	7	0.1276
Pure Error	0.67	2	0.33		
Cor. Total	593.73	14			

R^2= 0.9871, adjusted R^2 =0.9638, predicted R^2=0.8088, adequate precision= 20.276.

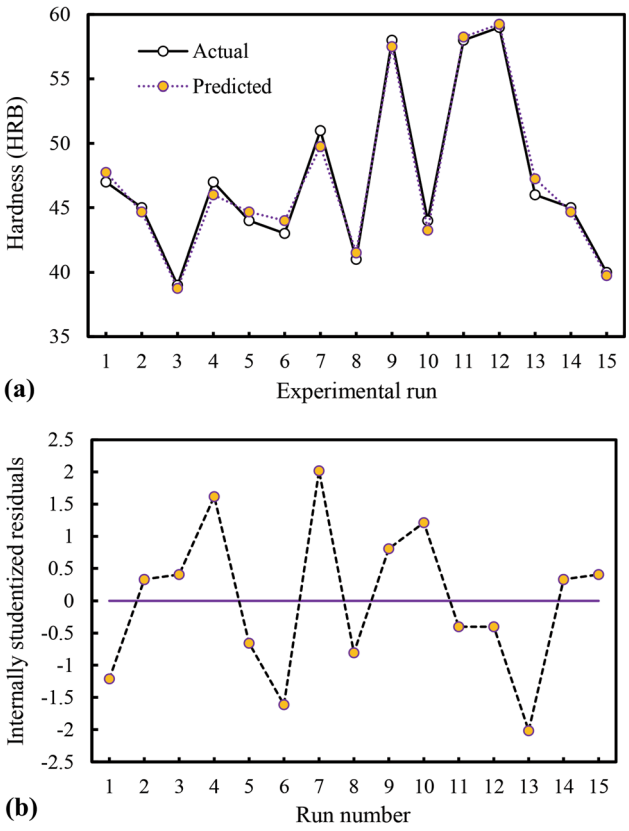

Fig. 10 (a) The comparison between actual and predicted values and (b) Residuals vs. run number for the hardness

contribution. The percentage effect of each factor was calculated from Eq 9 by using the results of ANOVA. The obtained results are illustrated in Fig. 12.

$$P(\%) = \frac{SS_i - (DoF_i \times MS_e)}{SS_T} \times 100 \qquad \text{(Eq 9)}$$

Figure 12(a) illustrates that some factors are more significant than others. It shows that the most significant parameters on grain size are holding time (53%) and reheating temperature (36%). The ECAP passes has a low impact (3%) on the grain size. The other parameters have affected the grain size by 8%.

Figure 12(b) indicates that the holding time, the reheating temperature, and the ECAP passes have the most effect on the shape factor by 45, 32, and 7%, respectively. Also, the effect of error and other parameters on the shape factor is about 16%.

The ECAP passes by 45%, the holding time by 27% and the reheating temperature by 17% have the greatest impact on the hardness of the samples at the semi-solid temperature. In this case, the influence of other parameters is about 11%.

It is shown in Fig. 12 that the other parameters have also influenced the grain size, shape factor and hardness values. These parameters have not been investigated in this study and they may be pressing speed, and temperature, the effect of friction, and other uncontrollable factors.

5. Conclusions

In this paper, the microstructural characteristics and mechanical properties of the 7075 aluminum alloy processed by the ECAP method were investigated in the semi-solid state through statistical methods. The effects of the ECAP passes, reheating temperature and holding time on the grain size, shape factor and hardness values were presented using RSM based on BBD. Three quadratic models have been developed for each of the responses. From the above investigations, some conclusions can be highlighted as follows:

- The results of ANOVA proved that the empirical models are adequate and they can predict the values of the responses close to those obtained experimentally with a 95% confidence interval.
- The grain size is mainly influenced by the holding time and the reheating temperature with the contributions of 53% and 36%, respectively. The interaction effect of reheating temperature and holding time is a significant factor with a slight impact, where the total percentage contribution of the interaction effects and other not considered parameters are about 8%.
- It can be seen that the number of ECAP passes; reheating

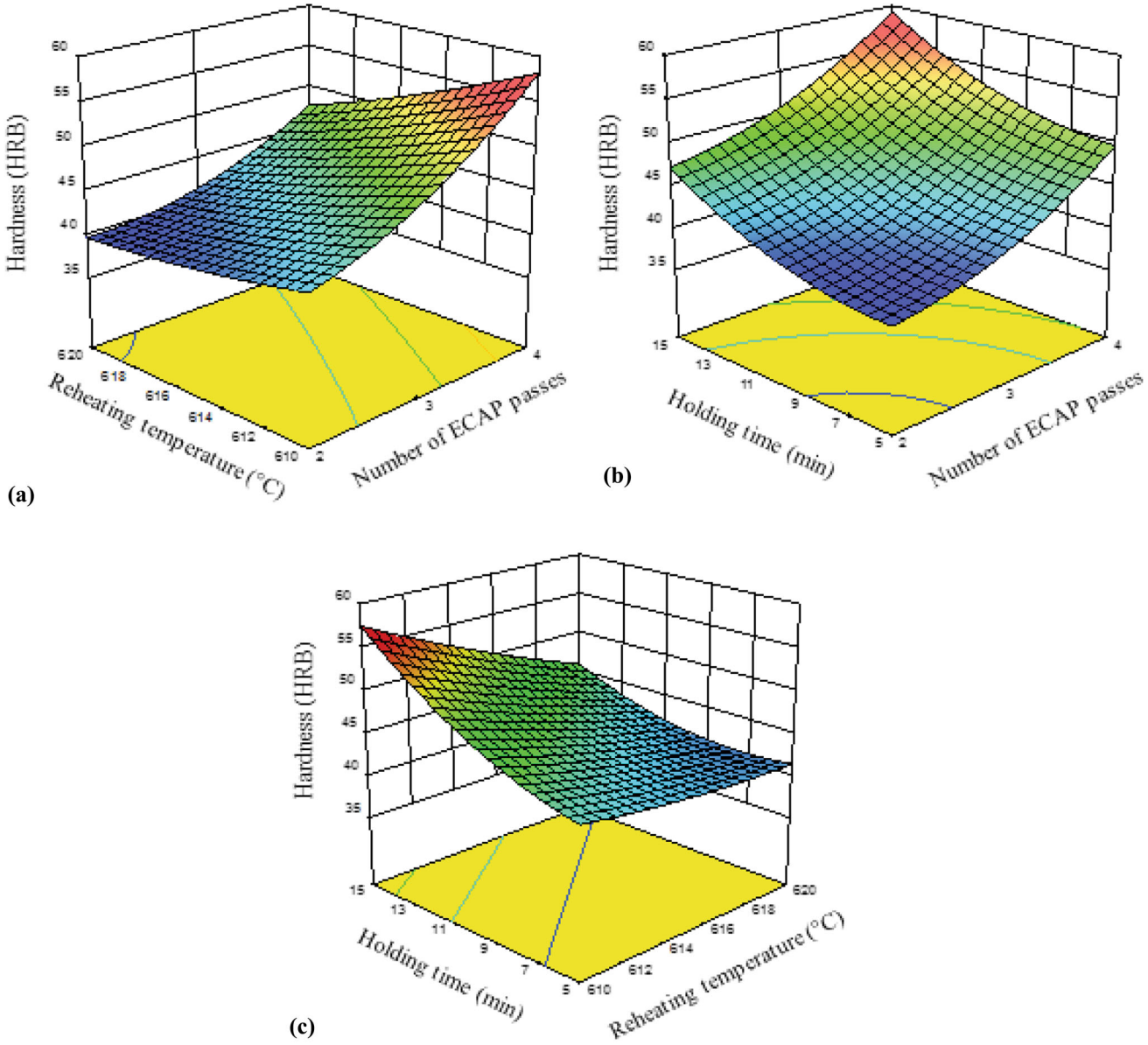

Fig. 11 Response surface plots showing the effects of (a) the number of ECAP passes and reheating temperature (b) the number of ECAP passes and holding time and (c) reheating temperature and holding time on hardness

temperature and holding time have statistical significance on the shape factor, where interaction between most factors has no significant effect except the number of ECAP passes and reheating temperature. The holding time, reheating temperature, and the number of ECAP passes by 45%, 32%, and 7% have the most effect on the shape factor, respectively. The effect of error and other parameters on the shape factor is 16%.

- It is observed from the ANOVA tables that all the three parameters and the interaction between the number of ECAP passes and reheating temperature along with the reheating temperature and holding time are significant parameters that affect the hardness values. Moreover, the number of ECAP passes had the most effect on hardness value (45%), followed by holding time (27%).
- The number of ECAP passes with statistical significance has a slight positive effect on the grain size and shape factor, whereas it contributes positively to the mechanical properties (hardness value).
- The semi-solid heat treatment parameters (reheating temperature and holding time) strongly affect the three examined responses. This indicates the sensitivity of the responses to the process parameters, which should be selected carefully.

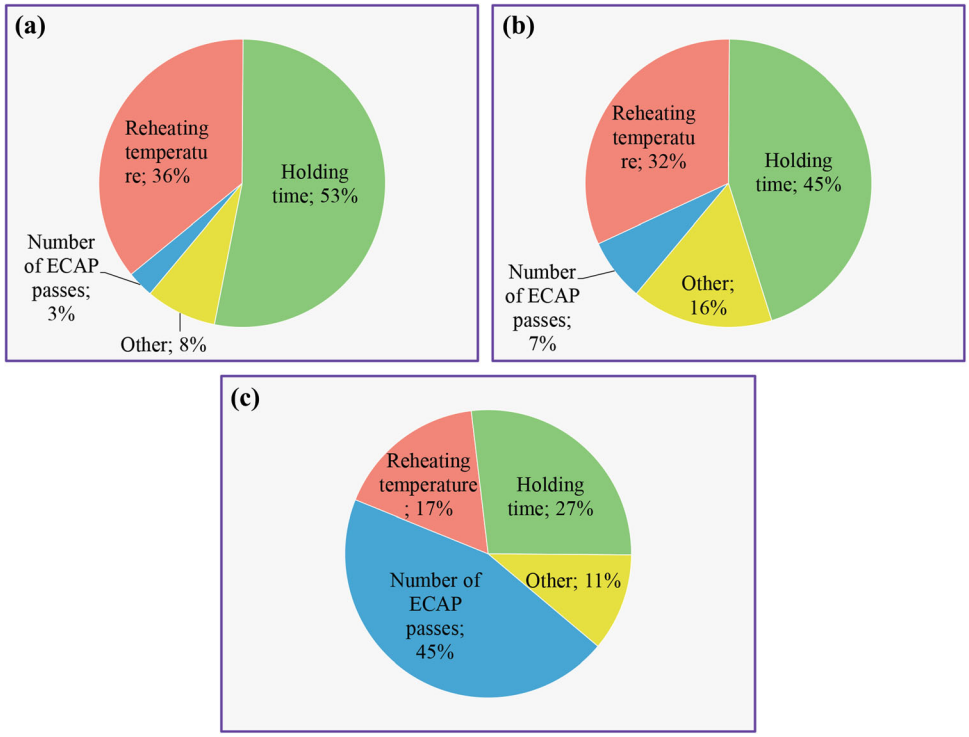

Fig. 12 Percentage contribution to (a) grain size, (b) shape factor and (c) hardness values

References

1. X. Luo, M. Wu, C. Fang and B. Huang, The Current Status and Development of Semi-Solid Powder Forming (SPF), *Jom*, 2019, **71**, p 4349–4361
2. G. Hirt and R. Kopp, *Thixoforming*, Wiley, New York, 2009
3. A. Pola, M. Tocci and P. Kapranos, Microstructure and Properties of Semi-Solid Aluminum Alloys: A Literature Review, *Metals*, 2018, **8**, p 181
4. F. Czerwinski, Thermomechanical Processing of Metal Feedstock for Semisolid Forming: A Review, *Metall. Mater. Trans. B*, 2018, **49**, p 3220–3257
5. F. Czerwinski, strain Induced Melt Activation (Sima): Original Concept, its Impact and Present Understanding, *Int. J. Cast Met. Res.*, 2020, **33**, p 157–164
6. E. Bagherpour, N. Pardis, M. Reihanian and R. Ebrahimi, An Overview on Severe Plastic Deformation: Research Status, Techniques Classification, Microstructure Evolution, and Applications, *Int. J. Adv. Manuf*, 2019, **100**, p 1647–1694
7. S.M. Hosseini, M. Roostaei, M. Mosavi Mashhadi, H. jabbari, and G. Faraji, Fabrication of Al/Mg Bimetallic Thin-Walled Ultrafine-Grained Tube by Severe Plastic Deformation. *J. Mater. Eng. Perform*, 2022
8. Z. Zhao, Q. Chen, Y. Wang and D. Shu, Microstructural Evolution of an ECAE-Formed ZK60-RE Magnesium Alloy in the Semi-Solid State, *Mater. Sci. Eng. A*, 2009, **506**, p 8–15
9. P. Vishnu, R.R. Mohan, E.K. Sangeethaa, S. Raghuraman and R. Venkatraman, A review on Processing of Aluminium and its Alloys Through Equal Channel Angular Pressing Die, *Mater. Today: Proc.*, 2020, **21**, p 212–222
10. M. Moradi et al., Recrystallization Behavior of ECAPed A356 Alloy at Semi-Solid Reheating Temperature, *Mater. Sci. Eng. A*, 2010, **527**, p 4113–4121
11. J.-L. Fu, H.-J. Jiang, and K.-K. Wang, Influence of Processing Parameters on Microstructural Evolution and Tensile Properties for 7075 Al Alloy Prepared by an ECAP-Based SIMA Process. *Acta Metallurgica Sinica (English Letters)*, 2017,
12. S. Ashouri, M. Nili-Ahmadabadi, M. Moradi and M. Iranpour, Semi-Solid Microstructure Evolution during Reheating of Aluminum A356 Alloy Deformed Severely by ECAP, *J. Alloys Compd.*, 2008, **466**, p 67–72
13. R. Meshkabadi, G. Faraji, A. Javdani and V. Pouyafar, Combined effects of ECAP and Subsequent Heating Parameters on Semi-Solid Microstructure of 7075 Aluminum Alloy, *Trans. Nonferrous Met. Soc. China*, 2016, **26**, p 3091–3101
14. L. Sang-Yong, L. Jung-Hwan and L. Young-Seon, Characterization of Al 7075 Alloys after Cold Working and Heating in the Semi-Solid Temperature Range, *J. Mater. Process. Technol.*, 2001, **111**, p 42–47
15. H.V. Atkinson, K. Burke and G. Vaneetveld, Recrystallisation in the Semi-Solid State in 7075 Aluminium Alloy, *Mater. Sci. Eng., A*, 2008, **490**, p 266–276
16. A. Bolouri, M. Shahmiri and E. Cheshmeh, Microstructural Evolution During Semisolid State Strain Induced Melt Activation Process of Aluminum 7075 Alloy, *Trans. Nonferrous Met. Soc. China*, 2010, **20**, p 1663–1671
17. A. Bolouri, M. Shahmiri and C. Kang, Study on the Effects of the Compression Ratio and Mushy Zone Heating on the Thixotropic Microstructure of AA 7075 Aluminum Alloy via SIMA Process, *J. Alloys Compd.*, 2011, **509**, p 402–408
18. A. Bolouri, M. Shahmiri and C.G. Kang, Coarsening of Equiaxed Microstructure in the Semisolid State of Aluminum 7075 Alloy Through SIMA Processing, *J. Mater. Sci.*, 2012, **47**, p 3544–3553
19. H. Mohammadi, M. Ketabchi and A. Kalaki, Microstructural Evolution and Mechanical Properties of Back-Extruded Al 7075 Alloy in the Semi-Solid State, *Int. J. Mater. Form.*, 2012, **5**, p 109–119
20. C.-P. Wang et al., Formation of Spheroidal Microstructure in Semi-Solid State and Thixoforming of 7075 High Strength Aluminum Alloy, *Rare Met.*, 2015, **34**, p 710–716
21. R. Meshkabadi, G. Faraji, A. Javdani, A. Fata and V. Pouyafar, Microstructure and Homogeneity of Semi-Solid 7075 Aluminum Tubes Processed by Parallel Tubular Channel Angular Pressing, *Met. Mater. Int.*, 2017, **23**, p 1019–1028
22. N.Q. Chinh et al., Developing a Strategy for the Processing of Age-Hardenable Alloys by ECAP at Room Temperature, *Mater. Sci. Eng. A*, 2009, **516**, p 248–252
23. A. Fallahi, H. Hosseini-Toudeshky, and S.M. Ghalehbandi. *Effect of heat treatment on mechanical properties of ECAPed 7075 aluminum alloy,* in *Advanced Materials Research*. 2014. Trans Tech Publ
24. R.Z. Valiev and T.G. Langdon, Principles of Equal-Channel Angular Pressing as A Processing Tool for Grain Refinement, *Prog. Mater Sci.*, 2006, **51**, p 881–981

25. D.C. Montgomery, E.A. Peck and G.G. Vining, *Introduction to linear regression analysis*, Vol 821 Wiley, New York, 2012
26. M. Rokni, A. Zarei-Hanzaki, H. Abedi and N. Haghdadi, Microstructure Evolution and Mechanical Properties of Backward Thixoextruded 7075 Aluminum Alloy, *Mater. Des.*, 2012, **36**, p 557–563
27. Y. Bin, W.-M. Mao and X.-J. Song, Microstructure Evolution of Semi-Solid 7075 Al Alloy Slurry During Temperature Homogenization Treatment, *Trans. Nonferrous Met. Soc. China*, 2013, **23**, p 3592–3597
28. B. Binesh and M. Aghaie-Khafri, Phase Evolution and Mechanical Behavior of the Semi-Solid SIMA Processed 7075 Aluminum Alloy, *Metals*, 2016, **6**, p 42
29. C. Tijun, L. Guoxiang, and H. Yuan, Microstructural evolution of equal channel angular pressed AZ91D magnesium alloy during semi-solid isothermal heat treatment. *Res. Dev.*, 2008,
30. N. Saklakoglu, I.E. Saklakoglu, M. Tanoglu, O. Oztas and O. Cubukcuoglu, Mechanical Properties and Microstructural Evaluation of AA5013 Aluminum Alloy Treated in the Semi-Solid State by SIMA Process, *J. Mater. Process. Technol.*, 2004, **148**, p 103–107